Meteorol. Atmos. Phys. 52, 183–203 (1993)

Meteorology and Atmospheric Physics

551.579.5

Department of Meteorology, Florida State University, Tallahassee, U.S.A.

Influence of Soil Moisture on the Sahelian Climate Prediction I

L. Bounoua* and **T. N. Krishnamurti**

With 10 Figures

Received February 2, 1993
Revised April 23, 1993

Summary

An energy balance based statistical parameterization of the soil moisture availability has been developed and implemented in the Florida State University Global Spectral Model to test its performance in long range prediction. Specifically, a soil moisture parameter based on a moisture budget analysis has been introduced to estimate the Bowen ratio. It is expressed as an evolutive function of the model predicted rainfall and surface temperature and takes into account some of the ground characteristics through its dependence on albedo and surface elevation. This scheme is used in conjunction with a prognostic equation for surface temperature to estimate the different energy fluxes at the surface.

A 42 waves triangular truncation global spectral model with 12 vertical levels has been used to perform parallel simulations, one of which includes the new planetary boundary layer parameterization. Seasonal simulations covering the onset and active phase of the West African monsoon have been carried out for the period between May and August 1979. A comprehensive comparison of the components of the surface energy balance between the two experiments has been carried out for different climatic regimes over the North African continent during the northern summer.

The new scheme appears to capture the essence of the surface layer physics in a simple formulation of the processes and has introduced an interesting description of the surface fluxes. Significant modulation of the surface temperature and its diurnal cycle amplitude were obtained. This was particularly evident over arid zones where extremely high surface temperatures were predicted by a simpler scheme.

An important and coherent interaction between the principal physical processes parameterized in the model has resulted from the introduction of the new scheme and has led to a better representation of the surface flux balance.

1. Introduction

The parameterization of the energy budget at the surface appears as one of the most important problems in modeling the planetary boundary layer (PBL). The influence of land surface processes on the atmospheric circulation has been extensively reviewed by many authors and it is widely agreed that over 70% of the energy driving the climate system is absorbed at the surface. Improvement in the radiative transfer calculations and utilization of similarity theory have had a positive impact in the estimation of the surface fluxes. Nevertheless, other non-measurable variables, such as the roughness length, the soil moisture availability and surface albedo, still constitute a serious obstacle when modeling the surface energy balance. At the simplest level, these parameters are globally and independently specified in many current general circulation models (GCMs). This parametrization appears far from describing any physical reality.

On the other hand, the new generation of GCMs include a biosphere-atmosphere transfer schemes (BATS), which have an explicit recognition of vegetation to describe the land-atmosphere interactions (Dickinson, 1984). The mean mor-

* Visiting Scientist from I.H.F.R, BP 7019. Seddikia, Oran, Algeria.

phological state of the vegetation is described as a function of time, and is used in the GCM to evaluate the exchange of heat, water vapor and momentum. Sensitivity studies (Sellers and Dorman, 1987) have shown that in these models, evapotranspiration is extremely sensitive to certain physiological properties of plants. It was then suggested that errors in the specification of the stomatal resistance could lead to uncertainties on the order of 7% in net radiation estimation and up to 25% in the calculation of the evapotranspiration flux. Furthermore, the BATS parameterization assumes that each grid element in the model is homogeneously covered by a single "big leaf", while the area represented by a grid square in the current GCMs averages approximately 250,000 km^2. At these spatial scales, large heterogeneties are observed in the topography, soil moisture, land use, vegetation, and precipitation which are all important elements for land-atmosphere interactions. It appears important, therefore, to design a land surface parameterization which describes the essence of the known physics in simple formulations of the processes.

Since the proposition of the albedo feedback hypothesis (Charney, 1975), many sensitivity studies using high performance GCMs have been carried out to assess the influence of land surface processes. In a comparative study of the effect of albedo change on drought in semi-arid regions, Charney et al. (1977) pointed out the sensitivity of Sahelian rainfall to changes in surface albedo. It was found that an increase in albedo caused a large reduction of rainfall in the Sahel region. It was then suggested that a positive surface albedo anomaly would produce cooling, subsidence and drying, which would consequently decrease the rainfall. Since then, several studies have focused on the role of land surface albedo on the influence of the atmospheric circulation, for example (Chervin, 1979; Henderson-Sellers, 1980; Carson and Sangster, 1981; Sud and Fennessy, 1982; Henderson-Sellers and Gornitz, 1984; Cunnington and Rowntree, 1986; Laval and Picon, 1986).

Idso and Deardorff (1978) pointed out the necessity for examining the role of soil moisture and its dependent evapotranspiration on climate. After the pioneering work of Manabe (1975) and Walker and Rowntree (1977) in numerically simulating the influence of soil moisture on the atmospheric circulation and rainfall, several studies using GCMs have examined the effect of soil moisture on seasonal circulation (e.g., Shukla and Mintz, 1982; Rind, 1982; Rowntree and Bolton, 1983; Yeh et al., 1984).

Other than soil moisture and albedo, surface roughness has also been shown to play an important role in land surface processes. Deardorff (1972) indicated that surface roughness is the principal parameter that can substantially affect the turbulent exchange coefficients and consequently influences the fluxes of heat, moisture and momentum. Sud and Smith (1984) showed that lowering the surface roughness to account for the smoothness of the desert had the effect of reducing the local rainfall. It is hypothesized that a decrease in the surface drag coefficient results in a suppression of the cross-isobaric moisture convergence into the desert.

It appears, therefore, that for arid and semi-arid regions, the primary influences on surface fluxes are: high surface albedo, dry ground, and small surface roughness due to the smoothness of the ground and absence of vegetation. Over such regions where evapotranspiration is generally small, particularly in summer, the net incoming radiation is mostly apportioned between outgoing longwave radiation (OLR) and sensible heat. An increase in surface albedo tends to decrease the energy absorbed at the surface, and consequently reduces all the fluxes. This cools the surface layer and induces compensatory heating via sinking motion aloft and divergence near the surface. These two effects result in a suppression of rainfall activity.

In contrast, increasing soil moisture does not significantly affect the surface radiation balance, but substantially decreases the Bowen ratio. The increase of evapotranspiration at the expense of sensible heating produces a cooler and moister planetary boundary layer (PBL) since the sum of latent and sensible heat must remain essentially the same. This will increase the PBL relative humidity, which is a key factor for the triggering of moist convection.

Finally, a reduction of the surface roughness would not change the surface radiation. Likewise the fluxes of heat and moisture would remain almost the same as for a rough surface. However, since a decrease in the surface roughness results in a reduction of the bulk energy transfer coefficients, it must be accompanied by larger gradients of temperature and specific humidity between the surface and the lowest PBL layer.

In this investigation a new algorithm for the determination of the Bowen ratio, which represents the central point in land surface parameterization, is implemented. Specifically, a ground wetness parameter based on the vertically integrated moisture budget is introduced. It is expressed as a function of the past 24 hour mean rainfall rate, surface temperature, as well as the surface albedo and terrain elevation to take into account the response of both the soil morphology and the climate forcing. This parameterization works equally well for short and long range prediction.

2. Modeling Strategies

The general equation governing the evolution of soil moisture without subsurface water transfer is expressed as

$$\frac{\partial m(z)}{\partial t} = N(z) - \frac{\partial M(z)}{\partial z}, \tag{2.1}$$

where $m(z)$ is the soil moisture content, $N(z)$ is the sink/source term of moisture, and $M(z)$ is the moisture flux defined as:

$$M_{\text{surf}} = (P + S_m - R_n - E)_{\text{surf}}. \tag{2.2}$$

The terms on the right hand side of (2.2) represent the precipitation, the snow melt, the runoff and the evaporation rates, respectively. The soil moisture availability is defined as the fractional soil moisture content at the surface:

$$GW = \left[\frac{m}{m_{\max}}\right]_{\text{surf}}, \tag{2.3}$$

where $m_{\max}$ represents the field capacity.

In the present Florida State University Global Spectral Model (FSUGSM), this parameter is prescribed at each Gaussian grid point using the following empirical formulation:

$$GW = 0.85(1.0 - \exp(-200(0.25 - \alpha)^2)), \quad \alpha \leqslant 0.25 \tag{2.4}$$

where α, the surface albedo, is constant in time. Furthermore, the ground wetness parameter is set to zero for land points having an albedo greater than 0.25 in the absence of ice or snow. The proposed scheme is based on surface moisture analysis following Nitta (1972) and Yanai et al. (1973). The moisture continuity equation, averaged over a horizontal domain, is written as:

$$\overline{\frac{\partial q}{\partial t}} + \overline{\nabla \cdot q\vec{v}} + \overline{\frac{\partial}{\partial p}(q\omega)} = e - c, \tag{2.5}$$

where c is the rate of condensation per unit mass of air, e is the rate of evaporation and q denotes the specific humidity. $\vec{v}$ is the horizontal wind and ω the p-vertical velocity. Assuming that small scale eddies in the horizontal components of the wind have no significant correlations with the eddy component of the specific humidity, (2.5) may be written as,

$$Q_2 \equiv -L\left(\frac{\partial \bar{q}}{\partial t} + \nabla\cdot(\bar{q}\vec{\bar{v}}) + \frac{\partial}{\partial p}(\bar{q}\bar{\omega})\right)$$

$$= L(c - e) + L\frac{\partial}{\partial p}\overline{q'\omega'}, \tag{2.6}$$

where the bars represent running horizontal averages and the primes stand for deviations from large scale. Hence Q_2 represents the large scale apparent moisture sink (Yanai et al., 1973). Upon vertical integration over the entire column one obtains:

$$\frac{1}{g}\int_{P_T}^{P_s} Q_2 dp = \frac{L}{g}\int_{P_T}^{P_s}(c - e)dp + \frac{L}{g}\int_{P_T}^{P_s}\left(\frac{\partial}{\partial p}\overline{q'\omega'}\right)dp, \tag{2.7}$$

where P_T is the pressure at the top of the column taken to be 125 mb and where the eddy moisture flux is assumed to vanish. P_s is the surface pressure. Upon integration, (2.7) then reduces to

$$\frac{1}{g}\int_{P_T}^{P_s} Q_2\, dp = LP_0 + \left(\frac{L}{g}\overline{q'\omega'}\right)_{p=ps}. \tag{2.8}$$

The surface latent heat flux is then obtained as:

$$LE_0 = LP_0 - \frac{1}{g}\int_{P_T}^{P_s} Q_2\, dp. \tag{2.9}$$

where P_0 is the amount of precipitation and E_0 is the rate of evaporation at the surface.

The large scale apparent moisture sink Q_2 has been evaluated using FGGE IIIB analysis (A list of acronyms is provided in Appendix 1). The vertical p-velocity, in the calculation of Q_2 has been obtained kinematically by integrating the mass continuity equation with a surface boundary condition taking into account the sliding motion along the sloping topography and assuming an adiabatic motion near the tropopause (Krishnamurti and Sheng, 1984). Once the large scale apparent moisture sink has been calculated, the latent heat flux at the surface is obtained using

(2.9). Next, the surface energy balance, coupled to the surface similarity theory, is solved for the soil moisture availability. At this point, it should be noted that the existing formulation of the surface energy balance in the FSUGSM assumes that the net incoming solar radiation absorbed at the surface is partitioned only between sensible and latent heat fluxes. In this study, the surface energy balance is treated using a soil-slab model following Blackadar (1979). A thin soil layer at surface temperature is assumed to be in thermal contact with a deeper layer at temperature T_m. The deep layer temperature, is taken as the lowest model level temperature averaged over the most recent past five days. The surface energy balance is then expressed as:

$$C_g \frac{\partial T_s}{\partial t} = (1-\alpha)SW\downarrow + LW\downarrow - \sigma T_s^4 - FS\uparrow - FL\uparrow - C_g K_m (T_s - T_m), \quad (2.10)$$

where C_g is the heat capacity per unit area of the slab and T_s designates the surface temperature. $SW\downarrow$ is the incoming shortwave radiation, α is the surface albedo and $LW\downarrow$ is the longwave radiative flux into the ground. The term σT_s^4 represents the OLR, where σ is the Stefan-Boltzman constant. FS and FL are the fluxes of sensible and latent heat, respectively. The last term in (2.10) is the heat flux carried into the ground.

Following Blackadar (1979), the heat capacity of the slab is described as:

$$C_g = 0.95(\lambda C_s / 2\Omega)^{1/2}, \quad (2.11)$$

where λ is the thermal conductivity of the soil, C_s is the heat capacity per unit volume and Ω is the angular velocity of the earth's rotation. K_m is given by:

$$K_m = 1.8\Omega. \quad (2.12)$$

In this formulation, C_s and λ are expressed as a function of the soil moisture availability and are written as:

$$C_s = (1.42 + 1.68 * GW) * 10^6, \quad (2.13)$$

$$\lambda = (0.25 + 1.33 * GW). \quad (2.14)$$

The incoming radiative fluxes are computed using the FSU radiative transfer model described by Krishnamurti et al. (1990). The latent heat flux is estimated from large scale observations using (2.9) and the sensible heat flux is expressed as:

$$FS = \rho C_h C_p |\vec{v}_2| (T_s - T_2), \quad (2.15)$$

where T_2 and $\vec{v}_2$ are the lowest model level temperature and horizontal wind, respectively. C_p is the specific heat of air at constant pressure and C_h is the heat turbulent exchange coefficient. Since C_s and λ depend on the ground wetness, a guess field of the latter is provided from climatology. Given a first guess surface temperature and ground wetness, the surface energy balance is solved for surface temperature. The saturation specific humidity at the surface $q_s(T_s)$ is next computed, and the stability dependent turbulent exchange coefficients, C_h and C_q, are estimated using similarity theory. Finally, the ground wetness is updated as:

$$GW = \frac{1}{q_s(T_s)} \left[q_2 - \frac{LE_0}{\rho C_q |\vec{v}_2|} \right]. \quad (2.16)$$

This iteration converges towards an energy balance in which the surface temperature is consistent with the surface fluxes, the ground wetness and the surface stability.

A diagnostic study was performed with this scheme using the FGGE IIIb data set for the periods 11 May through 16 May and 20 June to 28 June 1979. The horizontal domain used extended from 2.8° to 38.4° N and from 45.9° to 113.5° E. This domain was chosen principally because of data availability (Dastoor and Krishnamurti, 1991). Rainfall data were provided by the Summer MONEX data set. This diagnostic study enabled the computation of the soil moisture availability over the entire domain and period of analysis.

The next step consisted of using the soil moisture availability obtained from this procedure and expressing it as a function of the large scale variables using a statistical approach. The parameterization of the ground wetness is based on the fact that soil moisture availability is sensitive to climate variation as well as the morphology and type of the soil and their different interactions. In this context, a multivariate linear regression model has been used to diagnose the ground wetness, as:

$$GW = a_0 + a_1 R + a_2 T_s + a_3 \alpha' + a_4 H' + a_{11} R^2 + a_{22} T_s^2 + a_{33} \alpha'^2 + a_{44} H'^2 + a_{12} R T_s + a_{13} R \alpha' + a_{14} H' R + a_{23} T_s \alpha' + a_{24} T_s H' + a_{34} \alpha' H', \quad (2.17)$$

where R is the past 24 hour mean rainfall rate (mm/hr), T_s is the surface temperature (°K), and α'

and H' are, respectively, the normalized albedo and surface height fields,

$$\alpha' = \frac{\alpha_{max} - \alpha}{\alpha_{max} - \alpha_{min}}, \tag{2.18}$$

$$H' = \frac{H_{max} - H}{H_{max} - H_{min}}. \tag{2.19}$$

In order to optimize the number of predictors a screening regression technique using the best subset regressions has been applied. Several regressions have been tested with a varying number of predictors, and for each experiment all the subset regressions have been examined. It was found that a reasonable amount of variance is explained by 7 variables only, and that adding more predictors does not improve the fit significantly. Finally the equation used to parameterize the soil moisture availability reduced to:

$$GW = a_0 + a_1 R + a_2 T_s + a_3 \alpha' + a_4 H' + a_{11} R^2 + a_{33} \alpha'^2 + a_{44} H'^2, \tag{2.20}$$

where the regression coefficients are:

$a_0 = 3.131$ $a_1 = 0.484$ $a_2 = -0.009$

$a_3 = 0.143$ $a_4 = -0.329$ $a_{11} = -0.130$

$a_{33} = 0.162$ $a_{44} = 0.349.$

For example, a location characterized by an albedo value of 0.15, having a surface temperature of 20 °C and receiving 2 mm/day of rain, will experience a soil moisture availability of 0.77 if its elevation is at sea level and of 0.74 if the location is at 1000 meters above sea level. For this particular example, the soil moisture reaches saturation after approximately 18 mm/day of rain. The extreme values of albedo and terrain are those of the domain over which the regression has been performed.

In this formulation, the ground wetness parameter appears to be most sensitive to the rainfall and surface albedo. It has a correlation coefficient of 0.54 with the past 24 hour mean rainfall rate, which when used as a unique predictor explains about 29% of the total variance (See Table 1). The coefficient r-squared is the total explained variance expressed in percent, and is given by:

$$r^2 = 100(1 - \mathrm{SSE}/\mathrm{SST}), \tag{2.21}$$

where SSE is the error sum of squares and SST is the total sum of squares. The second most important predictor appears to be the surface albedo. It has a correlation coefficient of about 0.49 explaining 24% of the predicted variance.

Table 1. *Variance Explained by Each Variable When Used Individually for the Regression of the Ground Wetness*

r-squared	variable
29.185	R
24.403	α'
22.931	α'^2
8.454	Ts
7.164	R^2
2.950	H'
2.059	H'^2

The surface temperature presents a relatively weak correlation with the ground wetness (0.29) and explains approximately 8% of the total variance, while the past 24 hour mean rainfall squared has a correlation coefficient of 0.26 accounting for 7% of the variance. The terrain field appears to have the smallest effect on the soil moisture availability parameter. As a final subset regression, (2.20) represents the best fit to the data, explaining approximately 65% of the total variance with a multiple correlation coefficient of 0.81.

The ground wetness parameter as described by the old scheme (Eq. 2.4) and the new scheme (Eq. 2.20) have been plotted against the ground wetness obtained from the diagnostic study (Fig. 1). The new scheme appears to introduce an important improvement. An off line examination of the new ground wetness parameterization gave reasonable ranges of values over subtropical and tropical regions but seemed to slightly overestimate the ground wetness over arid zones. It is believed that this is related to the small number of data points with high albedo in the domain over which the regression has been performed. Measurements of evaporation following Gash et al. (1991) allowed, however, for the adoption of a correction function over the desert regions. Since the ground wetness parameter obtained from the new parameterization depends on the most recent past day rainfall only, the soil moisture is expected to sharply decrease the second day after the last occurrence of rain. Gash et al. (1991) showed that evaporation remains close to its potential for about one week after the last occurrence of rain. Then the evaporation rate falls; however, even after about five weeks some evaporation with rates

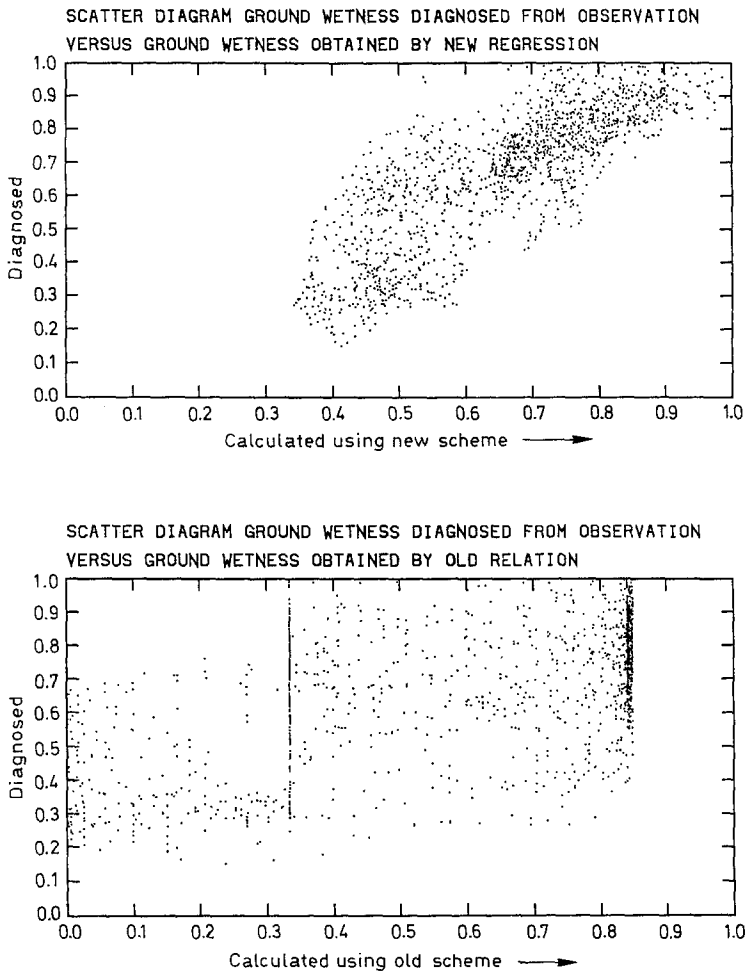

Fig. 1. Scatter diagram for soil moisture availability

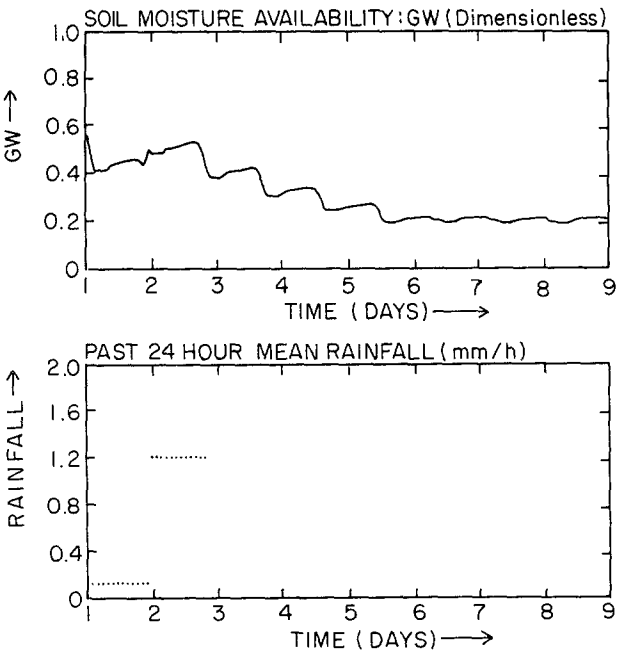

Fig. 2. Evolution of soil moisture availability as function of rainfall

of 1 to 2 mm/day were observed, suggesting extraction of water from deeper layers. The measurements of soil moisture deduced from gravimetric sampling showed that soil moisture availability decreases by about 40% of its saturated value in a period of approximately 5 days after a heavy rainfall. In this study, after each episode of rain producing more than 2 mm/day, a smooth decrease in soil moisture is allowed by taking 80% of the previous day value for a period of 5 days, but only if this newly computed ground wetness parameter is greater than the one that would be obtained in normal conditions (Fig. 2). This structure function is applied at each time step during the model integration, and hence, does not affect the soil moisture availability diurnal cycle.

Finally, the scheme is invoked only after the first 24 hours of integration, as the past 24 hour rainfall amount becomes available in the model. During the first day of forecast, a prescribed climatological field of ground wetness is used.

3. Experiments

The new algorithm for the soil moisture availability has been implemented in the FSUGSM to test its evolution and impact on the surface energy budget components during a long range weather prediction. Two parallel simulations are performed beginning 11 May and ending 31 August 1979 at 1200 GMT. In the first run (control), the ground wetness parameter as given by (2.4) is used in a surface energy balance which assumes the soil without heat capacity and therefore redistributes the incoming radiative energy between OLR, sensible and latent heat fluxes. The second experiment uses the new ground wetness parameterization as described by (2.20) together with a prognostic equation for surface temperature as expressed in (2.10).

In the control, the surface energy balance is solved iteratively using the Newton–Raphson iterative scheme. This method is first guess dependent and does not always converge. In the experiment, the solution of the surface energy budget is obtained using the bisection method with variable upper and lower limits to insure convergence. For both experiments, a ten day mean sea surface temperature is prescribed over the ocean.

The components of the surface heat budget have been monitored at a 2 hour time interval during the integration of the two experiments. This has been done at selected Gaussian grid-points located in areas of significantly different types of climatic regimes. Four points have then been chosen to fully describe the performance of the new scheme and to evaluate its influence on the different elements of the surface energy balance. All the points presented in the following discussion are located over longitude 0° E, but at different latitudes. The first point, for example, is located approximately at latitude 35° N and represents a Mediterranean type of climate. The second point (Point 2), located around 30° N over the northern Sahara represents a specific example of arid zones. The third point illustrated, is located around 18° N in the northern part of the Sahel region. The location of this point is of particular importance with respect to the monsoon rainfall. It is far north from the monsoon effect at the onset phase and generally receives most of its annual rain during the months of July and August as the monsoon progresses further north during its active phase. The fourth point, around 12° N, is characteristic of a tropical type of climate.

Since rainfall is the important factor controlling the soil moisture availability in the experiment, its response is outlined with reference to the components of the surface energy balance. The boundary between the earth and the atmosphere is extensively examined and a detailed surface energy budget analysis is carried out for the four months of the model integration. It should be noted that the integration concerned only 20 days during May.

4. Surface Energy Balance for the Month of May

4.1 Mediterranean Region

For the month of May, the point representing the Mediterranean region (Point 1) shows an almost constant net incoming radiation throughout the period of the forecast for the control (Fig. 3A). Although the difference between the new ground wetness parameter in the experiment and the prescribed one used in the control is not large, significant differences are observed in the surface energy budget components. In the control, the net incoming energy absorbed at the ground is partitioned only between the sensible and latent heat fluxes. Since the soil moisture availability is constant, the proportion of energy going into each flux component does not show significant variations (Fig. 3B, C). Except for changes due to atmospheric variables in the PBL, the fluxes of latent and sensible heat remain mostly the same during the model integration.

Not only has the new parameterization of the ground wetness altered the evolution of the latent and sensible heat fluxes in the experiment, but it has most importantly affected the Bowen ratio. Figure 3(B1, C1) show a decrease in both sensible and latent heat fluxes as compared to the control. This is associated with the introduction of the soil heat storage term in the surface energy balance. It appears that except for the diurnal variation due to its surface temperature dependence, the new ground wetness parameter does not depart much from that obtained using the empirical formulation in the absence of precipitation forcing for this location (Fig. 3E1). After a rainfall occurrence, however, the soil moisture availability undergoes significant changes which affect the entire energy

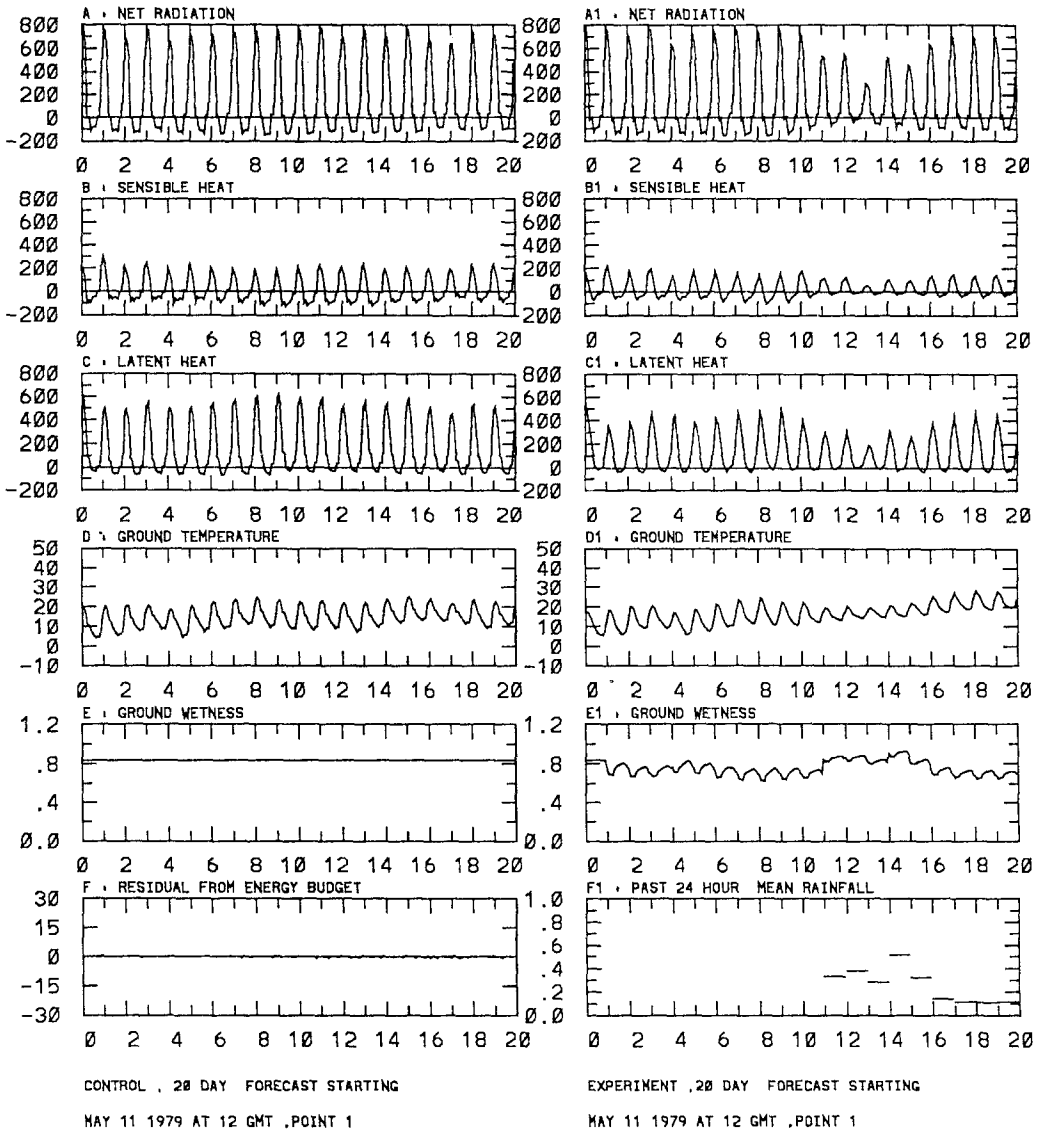

Fig. 3. Surface energy balance for Point 1, May, fluxes (Wm^{-2}), temperature (°C), rainfall (mm/h), ground wetness (dimensionless)

budget. For example, during day 10 the net radiative energy absorbed at the surface is approximately the same for both experiments. While in the control 770 Watt m^{-2} are absorbed at the surface, the experiment receives approximately 730 Watt m^{-2}. In the control, about 220 Watt m^{-2} is used as sensible and 550 Watt m^{-2} as latent heat due to the large ground wetness parameter. In the experiment, approximately 160 Watt m^{-2} goes into sensible heating and only 300 Watt m^{-2} is used in latent form. A decrease in the net incoming radiation, due to cloud cover during day 11, has reduced both the sensible and latent heat fluxes in the experiment. The repartition of energy into surface fluxes shows that in the control the Bowen ratio increases from 0.38 during day 10 to approximately 0.41 during day 11, while in the experiment this ratio decreases from 0.50 to 0.45 during the same period. It should be noted that between day 10 and 11, the control experienced a surface temperature increase of about 1 °C, whereas the reduction of the Bowen ratio in the experiment induced a moister PBL and decreased the surface temperature by about 2 °C during the same period. This is believed to have triggered moist convection and rainfall.

Convection and rainfall have the dual-effect of decreasing the total incoming solar radiation reaching the ground and increasing the soil moisture availability, which results in increasing the

latent heat flux at the expense of the sensible heat flux in the model. As a consequence, the amplitude of the surface temperature diurnal cycle decreases to maintain relatively low values during the following days. After the last day of substantial rain (day 15), an increase in the radiative heating, has led to a gradual increase in surface temperature and decrease in the ground wetness.

The energy partitioning in the two experiments has shown that the wetness of the soil is a central modulator of the surface fluxes. In fact, the surface temperature showed little difference between the control and the experiment during the first 10 days of the model integration. During the second 10 day period and just after the first rainfall occurrence, a net difference is observed in the temperature evolution as evidenced in Fig. 3(D, D1). The absence of a ground heat flux component in the control's surface energy balance has led to an overestimation of both sensible and latent heat fluxes. The prognostic equation for the surface temperature in the experiment, which has an explicit parameterization of the storage term, resulted in better description of all the fluxes. Therefore, even though the resulting surface temperature appears similar between the two experiments during the first 10 days of integration, the similarity is obtained by completely different means. In the control, the ground wetness parameter appears as a tunable parameter while it is diagnosed by the model at each time step in the experiment.

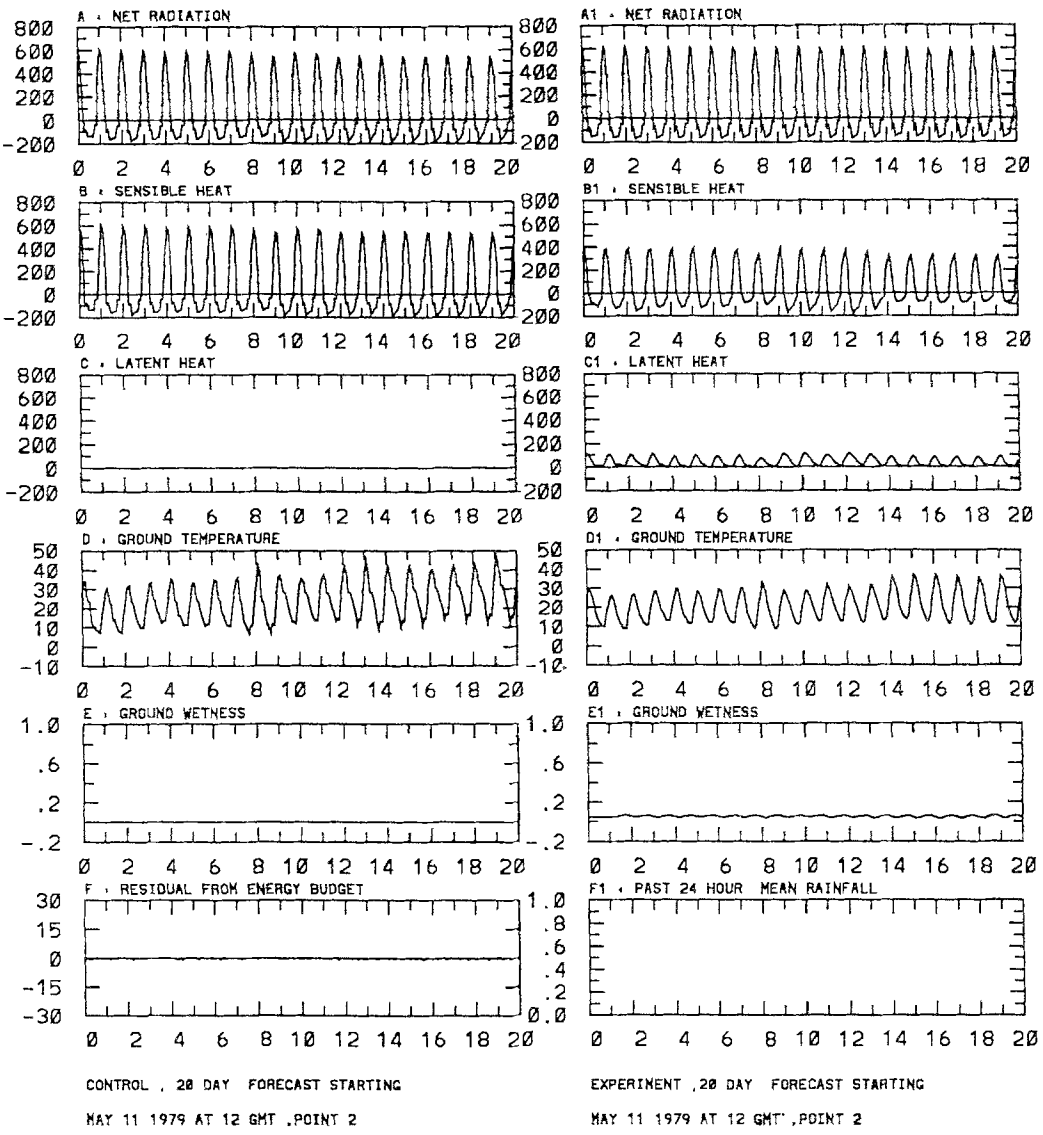

Fig. 4. Same as Fig. 3 but for Point 2

4.2 Arid Region

Figure 4 shows the surface energy budget for Point 2. Here, the net incoming solar energy is virtually identical between the control and the experiment since the region is cloud free during this period (Fig. 4A, A1). The partitioning of this energy, however, produces a remarkable difference between the two forecasts. The control sets the soil moisture availability to zero and therefore, does not allow for any exchange of latent heat (Fig. 4C). Consequently, the entire net radiative energy is transferred back to the atmosphere in the form of sensible heating (Fig. 4B). A large diurnal cycle is then observed in the surface temperature, with an amplitude as high as 34 °C during day 9 and a maximum temperature reaching 47 °C during the end of the month (Fig. 4D). The ground wetness parameter, obtained from the new scheme, appears reasonable for this location (Fig. 4E1), and its mean value around 5% is representative of a dry region. Even though small, this soil moisture availability allows a latent heat flux slightly less than 100 Watt m^{-2} and decreases the sensible heat flux relative to the control. It clearly appears that the introduction of a moisture component and the heat flux into the ground has contributed to a significant modulation of the surface temperature diurnal cycle amplitude. For instance, the amplitude of the diurnal temperature variation reduced to 24 °C during day 9 as compared to 34 °C in the control, with a maximum surface temperature around 37 °C.

At this point, it is worth noting that utilizing the so-called "bucket method" to estimate the potential evaporation assumes that the soil is saturated at the computed "skin" temperature. Over desert regions, where the soil is naturally dry, the surface temperature reaches high values during daytime. Therefore, using this temperature to calculate the saturation specific humidity at the surface can lead to an overestimation of evaporation. It has been suggested that the bucket method based on the bulk aerodynamic formulation cannot give a realistic representation of the complex land surface processes. Nevertheless, to verify the behavior of the new scheme, the components of the surface energy balance, as obtained from the two experiments are compared to those obtained by the global spectral model of the National Meteorological Center (NMC). The comparison is done for a selected point over the desert and for a 24 hour forecast starting 31 May 1979 (Pan, 1990). Table 2 displays the different components of the surface heat budget expressed in Watt m^{-2}.

Even though the two models have different physical parameterizations, the proportion of energy going into sensible and latent heat is quite similar between the NMC case and the experiment. It is therefore evident that setting the soil moisture parameter to zero results in an unrealistic heating of the PBL. It is also widely speculated that if some evaporation is allowed over the desert, this will cool and moisten the PBL and contribute to suppressing the dry convective mixing. Moist convection would then be enhanced and monsoon winds would penetrate deeper into the desert, supplying moisture farther north into the African continent.

4.3 Sahelian Region

For the Sahelian location (Point 3), the control's ground wetness parameter is much higher than the one obtained through the new parameterization (Fig. 5E, E1). This has inverted the partitioning of energy between sensible and latent heat fluxes, as compared to Point 2, and has introduced significant cooling at the surface. The experiment still shows that more energy is used in sensible form. However, an important part of the incoming radiation is utilized in latent form (Fig. 5C1). During this period, this location is still north of the influence of the West African monsoon and generally no rainfall is expected. In the control, the surface temperature reaches a maximum of

Table 2. *Comparison of Surface Fluxes Between NMC and FSU GSMs*

	Net radiation	Sensible heat	Latent heat	$\frac{\text{Sensible heat}}{\text{Net radiation}}$ (%)	$\frac{\text{Latent heat}}{\text{Net radiation}}$ (%)
NMC	430	190	50	44.2	11.6
FSU (exp1)	596	301	68	50.5	11.4
FSU (cont)	530	530	0	100	0

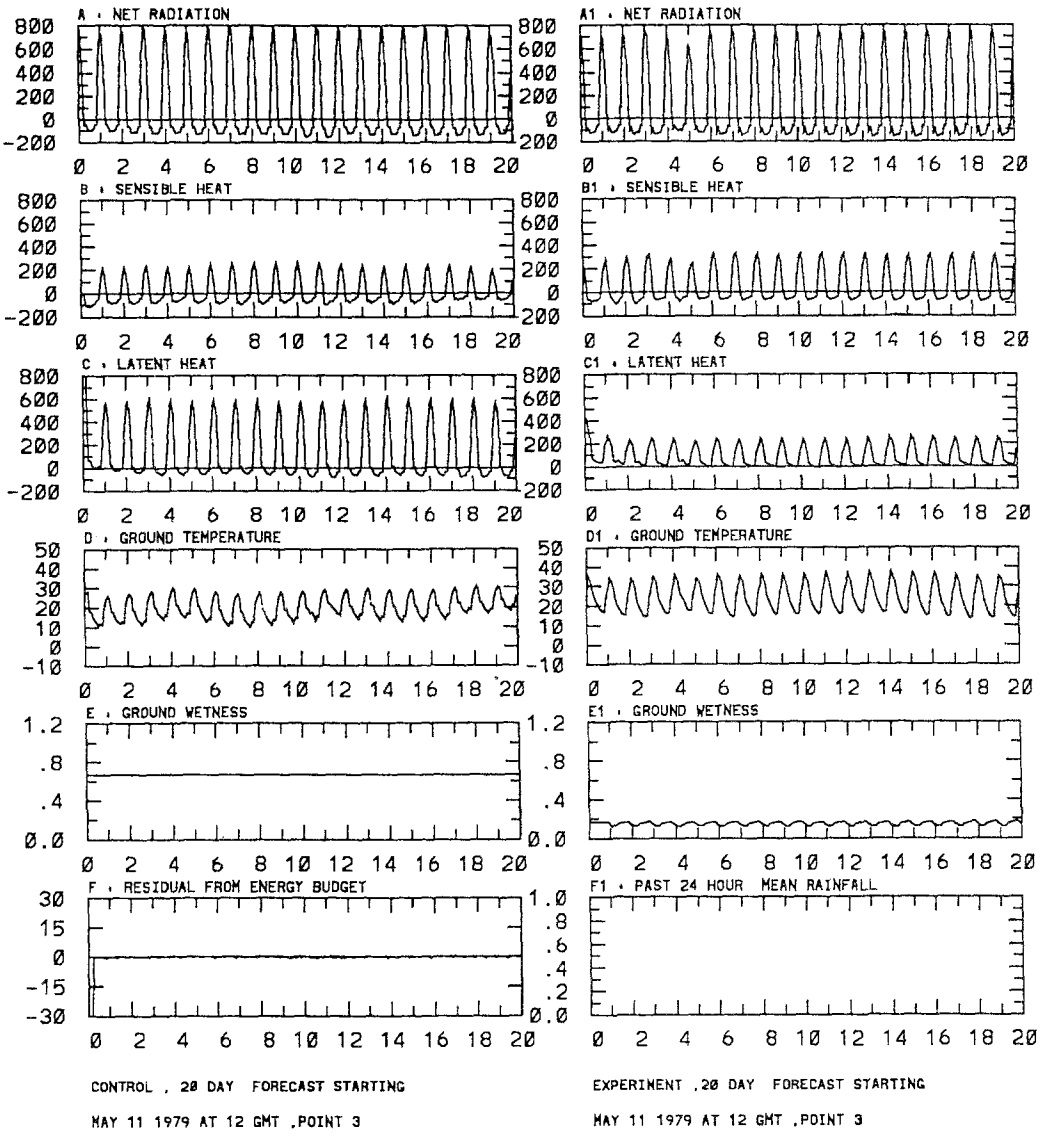

Fig. 5. Same as Fig. 3 but for Point 3

about 30 °C towards the end of the month. It reaches a maximum as high as 37 °C in the experiment, with more amplified diurnal ranges.

4.4 Tropical Region

Over the tropical region (Point 4), the control maintains a relatively high ground wetness parameter allowing an evaporation rate of 84% of the potential during the entire period (Fig. 6E). This results in a distribution such that the latent heat is approximately three times greater than the sensible heat (Fig. 6B, C). Since the sum of sensible and latent heat must balance the net energy absorbed at the surface, the radiative energy not used in latent form contributes to increase the temperature of the slab. Although the soil moisture availability allows more evaporation during the control, in which one would expect a cooler ground, the mean surface temperature at 1200 GMT is around 27 °C for both experiments. In the control, the surface temperature would normally have been lower than what is observed if some of the radiative energy had been transferred into the ground reservoir. It appears, then, that in the control's surface energy balance formulation, the excess of energy resulting from the absence of the storage term is compensated for by an excess cooling due to abnormally high evaporation rates. The surface temperature in the control has a

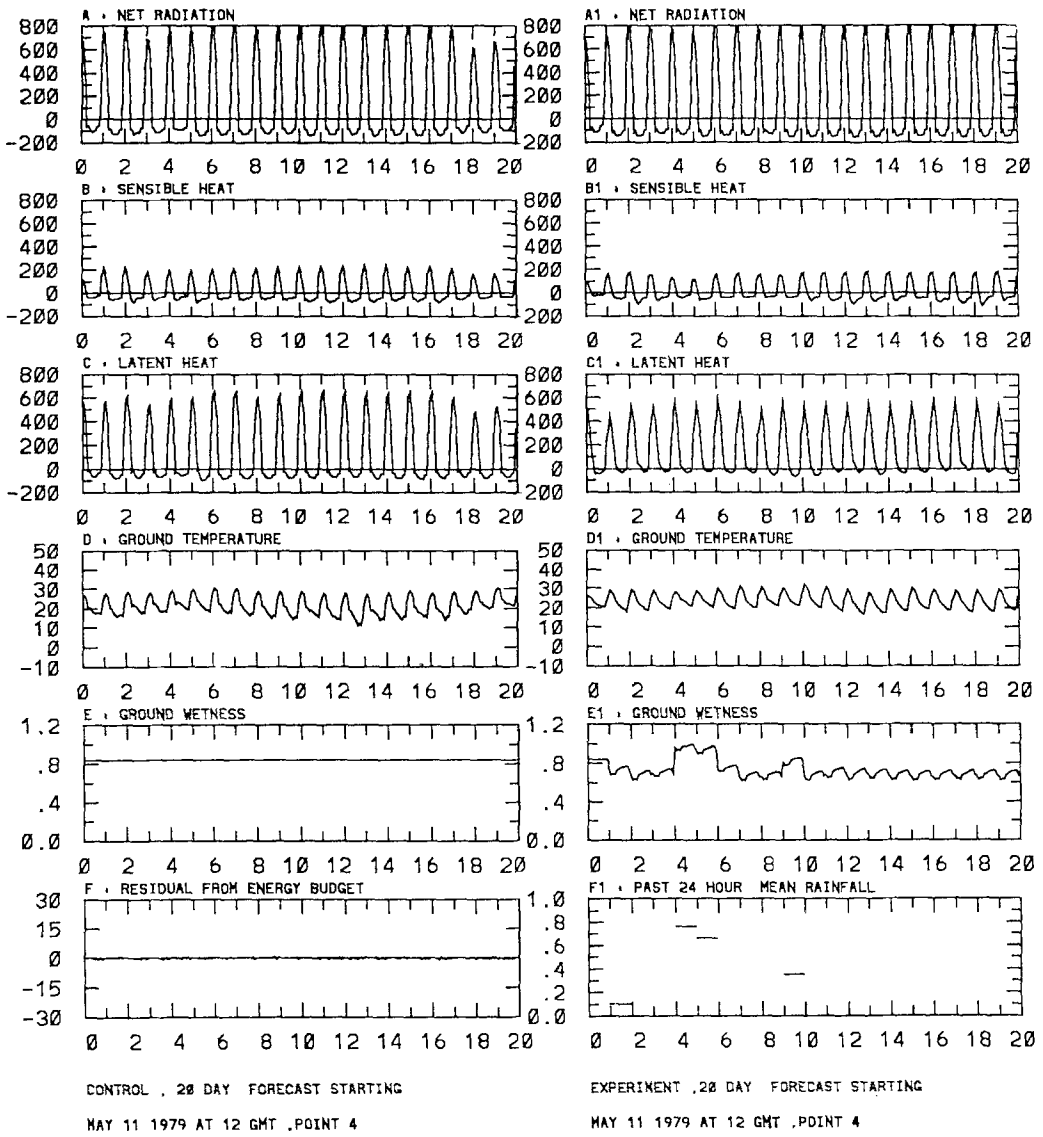

Fig. 6. Same as Fig. 3 but for Point 4

maximum of approximately 30 °C for most of the period except between the 11th and the 17th days of integration, when a decrease of about 3 °C in both maximum and minimum is observed (Fig. 6D).

For the same point, the variation in the soil moisture availability introduced by the new scheme is significant. Apart from the first 24 hours of the forecast when the ground wetness is identical to that of the control, the new formulation produced a soil moisture availability of about 0.74 in the absence of rainfall. It is important to note that this value, about 0.1 less than that used in the control, has produced an overall decrease in the evaporation rates. A sequence of rainfall between days 3 and 4 has, however, increased the soil moisture to its saturation level during the early morning hours of day 5, when the daily minimum temperature is observed. The rainfall observed during day 4 is associated with a decrease in the Bowen ratio. In fact, between days 3 and 4, the 1200 GMT sensible heat flux has decreased from 150 to about 125 Watt m^{-2}, while the latent heat flux has increased from approximately 409 to 483 Watt m^{-2}. This has decreased the Bowen ratio from 0.37 to 0.26 and appears to be responsible for moist convection. The use of the past rainfall in the new parameterization, has led to a significant increase in the soil moisture availability during day 5, which has enhanced the evaporation flux and

consequently the rainfall. Even though there is no evidence to support it, it appears that the rainfall, which occurred during day 5 in the experiment, would not have been produced, or would have been less, if the soil moisture availability was climatologically prescribed. Although no rainfall has been produced by the model during day 6, the value of the soil moisture availability during the next day is still higher than what would have been obtained under no rainfall stress. Through its structure function, the new parameterization allows for a slow drying of the ground after a rainy day. Unlike the control, the surface temperature showed a regular variation between approximately 20 °C and 30 °C during the entire forecast period, with a mean value of approximately 27 °C at 1200 GMT.

5. Surface Energy Balance for the Months of June, July and August

The surface energy balance for the months of June, July and August shows interesting aspects of the new soil moisture availability scheme and its effects on the rainfall. This is especially evident over sub-Saharan areas where monsoon surges started going far enough north to reach the Sahelian regions. Since the albedo is time independent for both experiments, the soil moisture availability remains constant in the control, and the proportion of energy available as latent heat

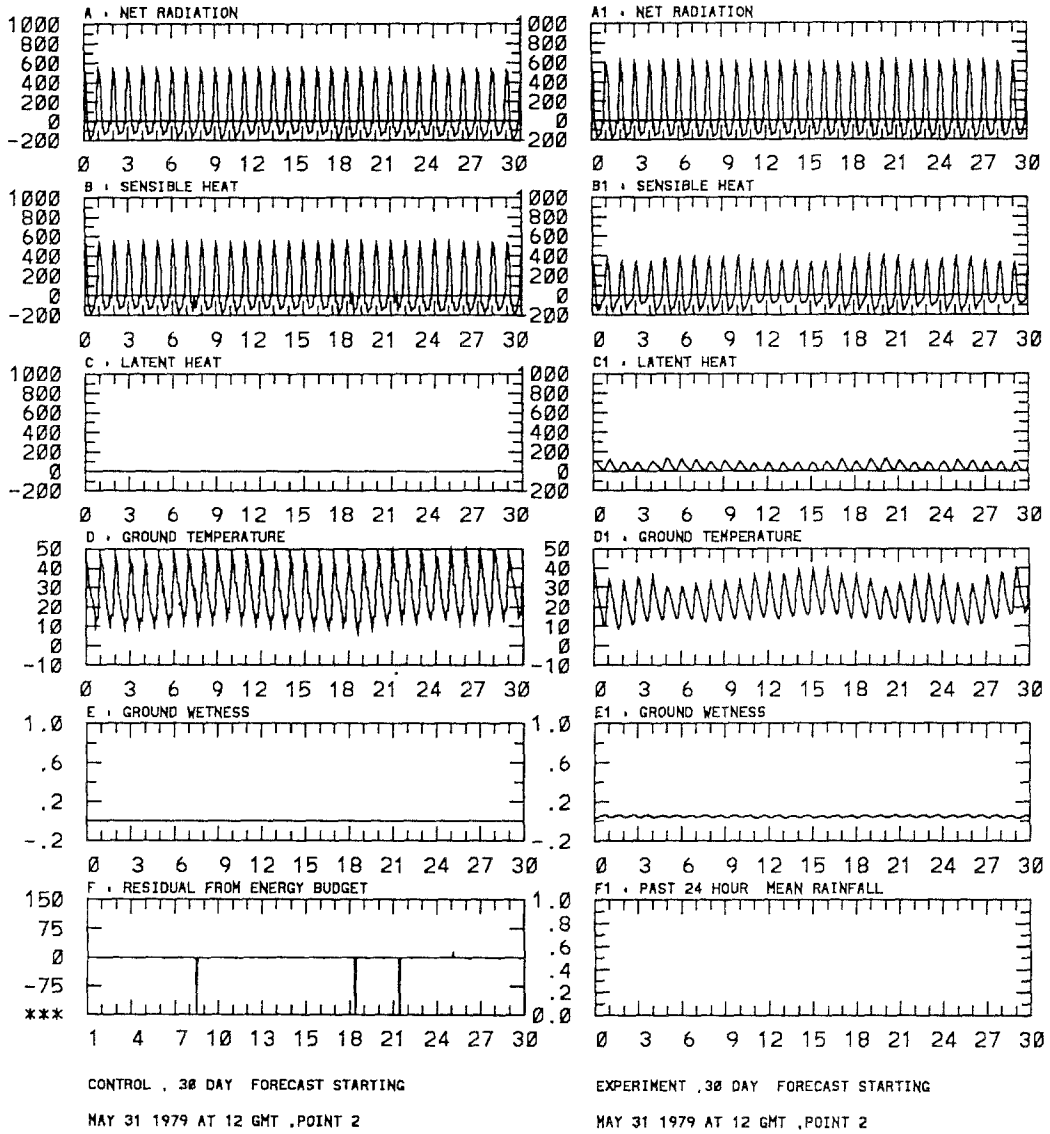

Fig. 7. Surface energy balance for Point 2, June, fluxes (Wm^{-2}), temperature (°C), rainfall (mm/h), ground wetness (dimensionless)

is unaffected regardless of any change that may occur at the surface. Therefore, the following discussion focuses on selected points for selected months which present relevant characteristics of the new parameterization. However, aspects that have not been covered in the previous section will be reviewed for the control.

5.1 Arid Region

The surface energy components for the desert point during June do not present important variations as compared to those of the month of May. For both experiments, an increase in the surface temperature consistent with the radiation is observed (Fig. 7D, D1). In the control, where evaporation is completely suppressed, diurnal cycle amplitudes in excess of 37 °C and high surface temperatures greater than 50 °C, are observed. During the daytime, about 600 Watt m^{-2} is transferred from the desert surface to the PBL in the form of sensible heating (Fig. 7B). The sensible heat is carried by the eddies in the unstable PBL which lead to cooling and stabilization of the surface layer.

The residual from the energy budget at the end of the iteration procedure in the control is shown in (Fig. 7F). As stated earlier, the Newton–Raphson iterative technique used in the control is first guess dependent and does not always converge. Therefore, only a limited number of iterations are permitted when solving for the surface energy balance. Although the surface temperature is relaxed towards its first guess value in case of non-convergence, the sensible heat flux shows errors on the order of 150 Watt m^{-2} (Fig. 7B). This problem is avoided in the experiment, where an iterative scheme based on the bisection method with variable limits is being utilized.

As for the month of May, the ground wetness parameter obtained through the new scheme for Point 2 is small for this dry, high albedo region (Fig. 7E1). Nevertheless, the energy budget apportions about 100 Watt m^{-2} as latent heat flux and 350 Watt m^{-2} as sensible heat flux at the time of maximum insolation. The rest of the net incoming energy serves partially to balance the storage term and force the surface temperatue variation. The overall effect of the new surface energy balance is that of cooling the surface layer. Unlike the control, the surface temperature shows an evolution with moderate diurnal cycle amplitudes of around 23 °C, and an absolute maximum temperature of 40 °C. For comparison, one can mention that Blake et al. (1982), using aircraft measurements over the Arabian desert, estimated an upward sensible heat flux of 250 Watt m^{-2} at 1000 hPa. Furthermore, the ground temperature, as measured by onboard instruments, showed a diurnal fluctuation of about 25 °C, with a maximum temperature of 44 °C. It was also found that the area averaged specific humidity over the Empty Quarter had a mean value close to 5 g/kg during the daytime, suggesting that the PBL is not completely dry.

During the summer season, the arid region is characterized by almost invariant atmospheric conditions, dominated by clear sky and warm, dry air. This is due to its location far south from the influence of the Mediterranean Sea, and far enough north to escape the West African monsoon. The only variation observed is therefore in the solar radiation flux, which increases with the progression of the summer season. For both experiments, the increase in radiative energy has led to a significant increase in the surface temperature during July and August (not shown). During these two months the control resulted in extremely high surface temperature exceeding 50 °C on many occasions, with a typical diurnal cycle amplitude of 35 °C. On the other hand, the experiment predicted surface temperature maxima ranging between 40 and 44 °C with a diurnal range of 24 °C. The surface temperature evolution as predicted using the new surface energy balance during these two months appears to be in better agreement with the measurements obtained by Blake et al. (1982), while it is overestimated by more than 6 °C in the control. A point to stress, however, is that although the new parameterization of the soil moisture availability is not complex and time consuming, it nevertheless introduced a skillful representation of the main components of the surface energy budget.

5.2 Sahelian Region

The following section describes the gradual seasonal evolution of the various components of the surface heat budget. For reasons of commodity, the discussion is presented on a monthly basis.

5.2.1 Surface Budget During June

The Sahelian point shows that during the first 25 days of June, the ground wetness parameter simulated by the experiment allows daily evaporation rates ranging between 12 and 17% of the potential (Fig. 8E1). During this period, from a net absorbed radiation of approximately 750 Watt m^{-2}, about 300 Watt m^{-2} goes into sensible heating while 250 Watt m^{-2} is used as latent heat, maintaining a high Bowen ratio of 1.2 over the region.

Although there is no evidence to support it, the decrease in the net radiation during June 26 appears to be produced by cloud cover due to moisture advection from the monsoon region (Fig. 8A1). The basis for the above statement is that, previous to this day, the Bowen ratio was kept high, suggesting a dry and warm PBL. Since the relative humidity plays an important role in triggering convection, a dryer PBL below the convective cloud base cannot be expected to support moist convection. It is also believed that this moisture advection has produced the first monsoonal rainfall over the region.

Due to the substantial rainfall, the soil moisture

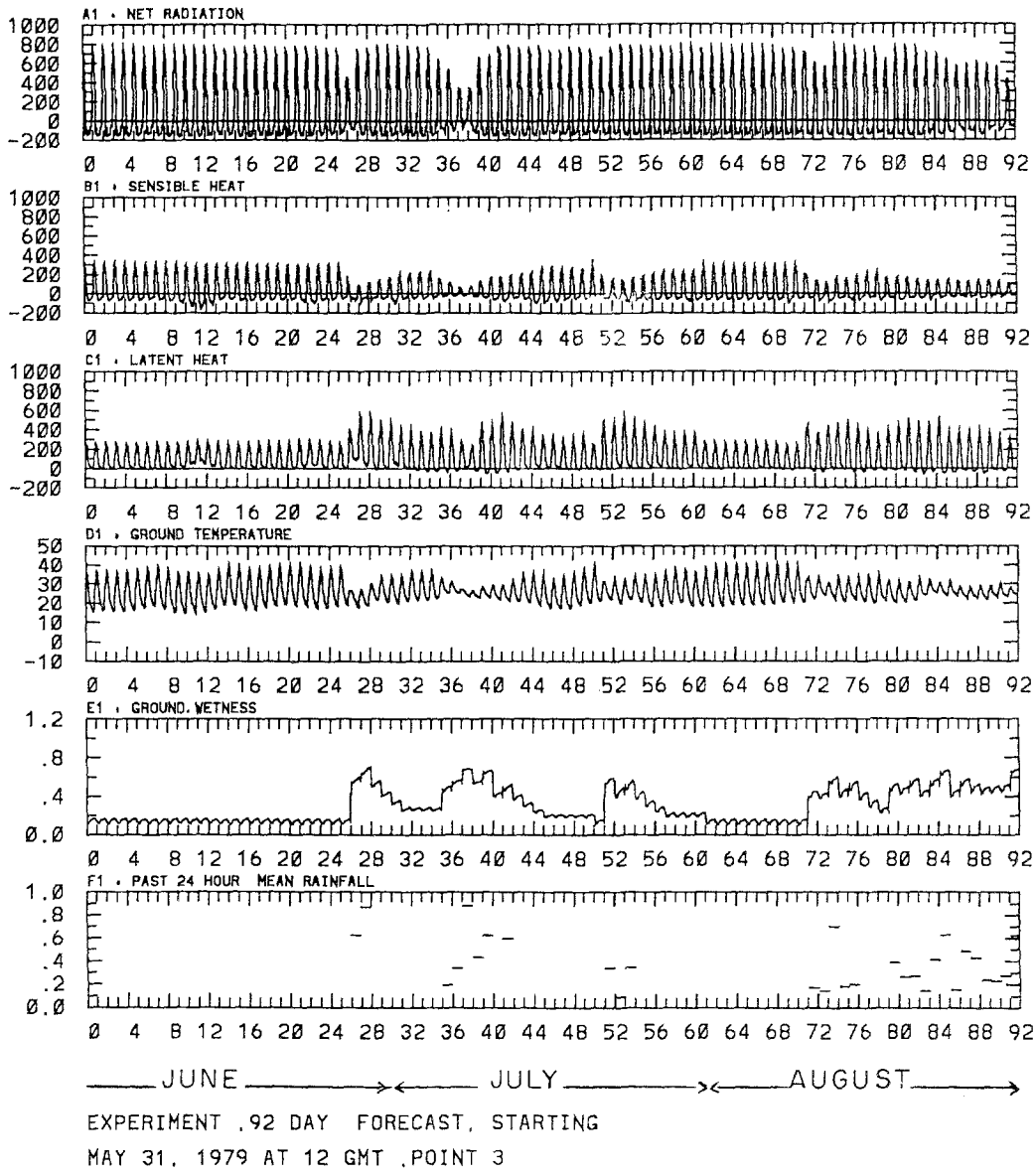

Fig. 8. Surface energy balance for the experiment Point 3, June, July, August, fluxes (Wm^{-2}), temperature (°C), rainfall (mm/h), ground wetness (dimensionless)

availability undergoes a sharp increase during day 27 producing a strong reversal in the surface fluxes distribution. For instance, the Bowen ratio decreases from 1.37 on the 25th at 1200 GMT to 0.27 the next day. This has further enhanced surface evaporation and has produced more rainfall on the 27th. The surface temperature presented regular fluctuations with diurnal cycle amplitudes of about 20 °C and maxima varying between 38 °C and 40 °C during the first 25 days. After that, it experienced a sharp cutoff, due to an increase in evaporation, reducing the maxima to between 25 °C and 32 °C during the last 5 days of June (Fig. 8D1).

5.2.2 Surface Budget During July

During July, the first four days of the experiment presented a relatively high Bowen ratio in excess of 0.7, characterizing a warm and dry PBL with surface temperatures reaching 37 °C. A decrease in the Bowen ratio from 0.80 to 0.47 is observed between day 4 and 5, when approximately 5 mm of rain is observed. The rainfall significantly affects the soil moisture availability, which shows an increase from 0.28 to 0.54 between day 5 and 6 (Fig. 8E1). This further enhances the surface evaporation, transferring more moisture into the PBL and decreasing the sensible heat flux. Due to the greater absorption of incoming solar radiation by water vapor, less radiative energy reaches the ground. A decrease from approximately 622 to 532 Watt m^{-2} is observed between day 5 and 6 (Fig. 8A1). Unlike the control, where a decrease in the incoming solar energy is accompanied by a reduction in both latent and sensible heat, in the experiment it affects mostly the sensible heat since the ground wetness remains high. As a result, the surface temperature dropped by about 1.5 °C and the model produced approximately 8 mm of rain during day 6. It should also be noted that both a decrease in surface temperature and an increase in rainfall contribute to an increase in the soil moisture availability. For instance, during the next day the ground wetness increased from 0.54 to 0.68 resulting in a decrease of surface temperature from 31 °C to 27 °C and 20 mm of rainfall. This feedback between land surface processes, radiation and moist convection continues until the model condenses the available moisture above the saturation level. At this point, the solar radiation reaching the ground increases again and drives the model towards a new state of equilibrium.

After each sequence of rainfall in the experiment, the scheme allows a smooth transition of soil moisture from the last value obtained with rainfall forcing to its climatological value in a period of five days. It is important to note that if the scheme were not to consider the previous state of the ground in the estimation of the soil moisture, a sharp decrease in the ground wetness, from approximately 0.50 to 0.20, would have occurred one time step after the 12th day of July and would have produced an increase in the surface temperature of about 5 °C in 20 minutes. This would be unrealistic if the last value of the ground wetness during the rainy period were at its saturation level.

5.2.3 Surface Budget During August

It is clear that the new parameterization of the soil moisture, especially through its past rainfall dependence, plays an important role in the precipitation distribution. In fact, a detailed examination of the soil moisture availability and the rainfall distribution reveals that just after the first rainfall occurrence during August, the ground wetness increases to more than twice its climatological value obtained in the absence of precipitation. This forces the model to convert approximately twice as much energy into latent heat, supplying therefore to the atmosphere the necessary ingredient for most convection. It should be noted that if the soil moisture were prescribed to some climatological value over this region, it would have underestimated the latent heat flux and then the precipitation if its value were too small, or overestimated them if the value were too high. If a constant climatological value of about 0.2 was prescribed for this location, it would have given a fair representation of the different surface fluxes and their related rainfall during the first 10 days of August. During the remaining period, however, it probably would have failed to simulate any of the observed rainfall. If the constant is tuned to produce the observed summer rainfall over the region, it would necessarily overestimate it during drier periods. It appears, therefore, imperative to allow the model to predict the soil moisture availability as a function of the prevailing surface conditions in order to provide a realistic interac-

tion between the different energy fluxes at the model's land-atmosphere interface.

The slow drying of the ground after a rainy period, introduced in the new parameterization, is quite important for the rainfall distribution. It can be argued that the rainfall produced by the model between August 17 and 18 would not have occurred if the soil moisture were simply relaxed to its climatological level after the last day of rain. The use of this technique has permitted more evaporation than would have normally been observed if the climatological value of the soil moisture were used immediately after the rainfall occurrence.

As a response to the surface fluxes distribution during August, the surface temperature in the experiment shows a diurnal variation of 20 °C with maxima around 40 °C during the first 9 days, corresponding to the dry episode. During this period, the sensible heat flux was maintained around 300 Watt m^{-2}, while the latent heating accounted for 250 Watt m^{-2} and the soil had an absorption of approximately 120 Watt m^{-2} at the time of maximum insolation. During day 10, the partitioning of the energy had been inverted as the sensible heating became less than 200 Watt m^{-2} and the latent heat more than 400 Watt m^{-2}. The soil heat flux remained almost at the same value,

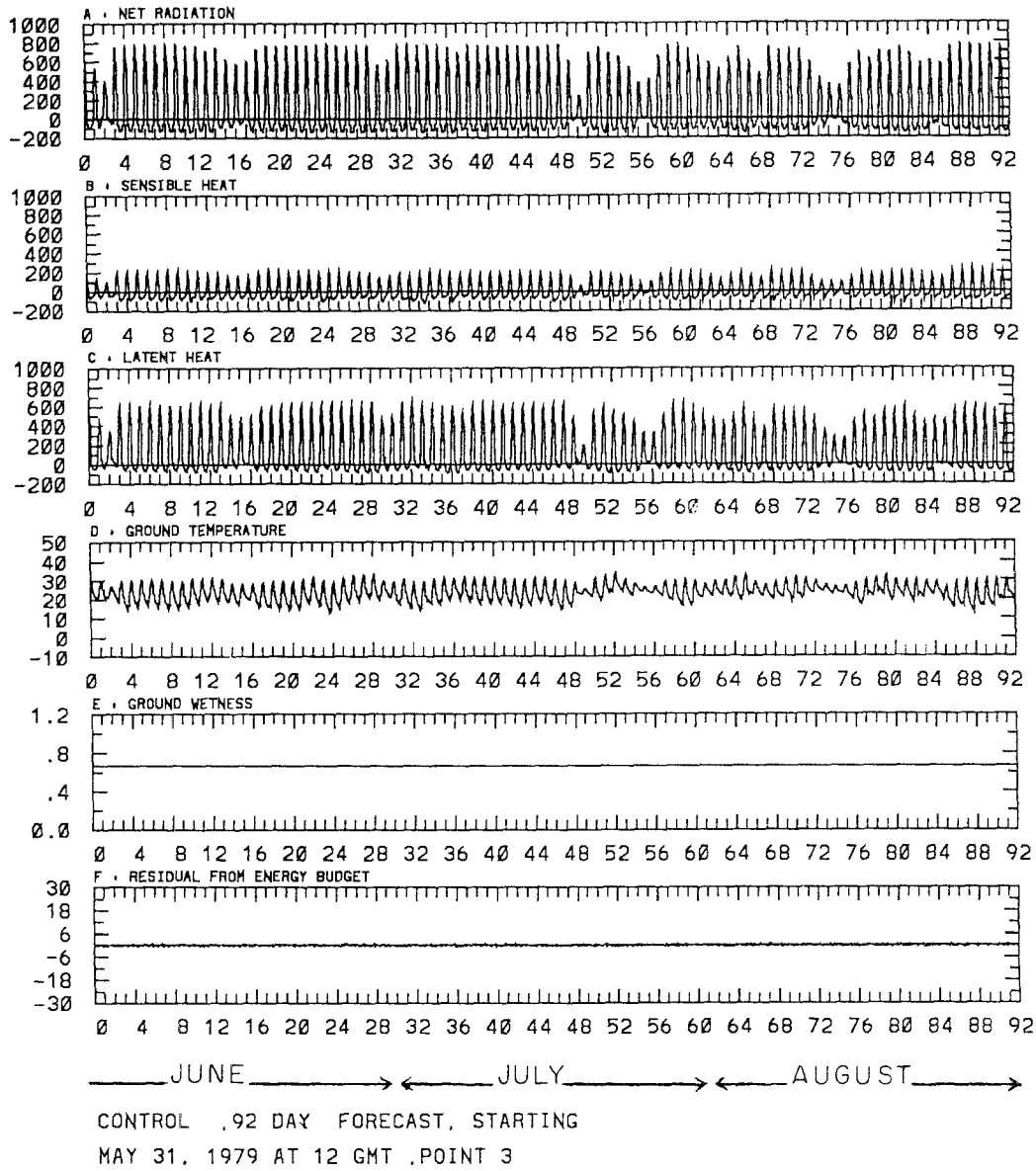

Fig. 9. Same as Fig. 8 but for the control

implying that the new partitioning of the energy contributed to an increase in the latent heat mostly at the expense of the sensible heat. This reduced the Bowen ratio and increased the relative humidity in the PBL. Consequently, the surface temperature maximum dropped by about 10 °C.

The control, with a constant soil moisture parameter of 0.66, resulted in an excessive moistening of the PBL (Fig. 9). However, the non-negligible amount of energy going into sensible heating kept the PBL from cooling too much. This distribution of the energy into surface fluxes is likely to produce more rainfall than the experiment. The excess of surface evaporation resulted in cooler surface temperatures during the entire period as compared to the experiment.

As previously mentioned, the location of Point 3, is quite interesting for the examination of the monsoon rainfall evolution over the West African region. In fact, during the month of May no rainfall was observed over this region and except for 2 days towards the end of the month, June was also virtually dry. It is believed that this limited rainfall during June is due to monsoonal surges which may occasionally bring moisture as high as 20° N even when the climatological position of the ITCZ is still around 15° N (Fig. 8F1). The meridional migration of the ITCZ is prominent during the month of July, when substantial rainfall was recorded at this location. It is also observed that the amount of rainfall recorded during a single week of July is greater than that of May and June combined. The rainfall distribution, however, presents a good representation of their episodal character showing an alternation between wet and dry periods. Although the occurrence of rain has increased during the month of August, corresponding to the maximum monsoon activity, it is important to note the dry spell of about 20 days before the first rain, and a shorter one of 4 days separating the two major rainfall episodes.

The discontinuous character of the rainfall over this region reveals that the monsoon is not well established. One may speculate, however, that a possible cause of this phenomenon is that this location is reached by monsoonal winds only when they overshoot the equilibrium position of their meridional oscillatory movement. Only then, the depth of the monsoon moisture layer becomes substantial, and rainfall may occur. The dry spells are believed to be associated with the withdrawal phase of the monsoon surges.

6. Feedback Processes

The use of the new soil moisture availability has introduced a complex feedback between the model physical mechanisms (Fig. 10). Over land, the sum of latent and sensible heat is mostly governed by the net radiation absorbed at the surface. The distribution of energy between these two fluxes is, however, strongly affected by the

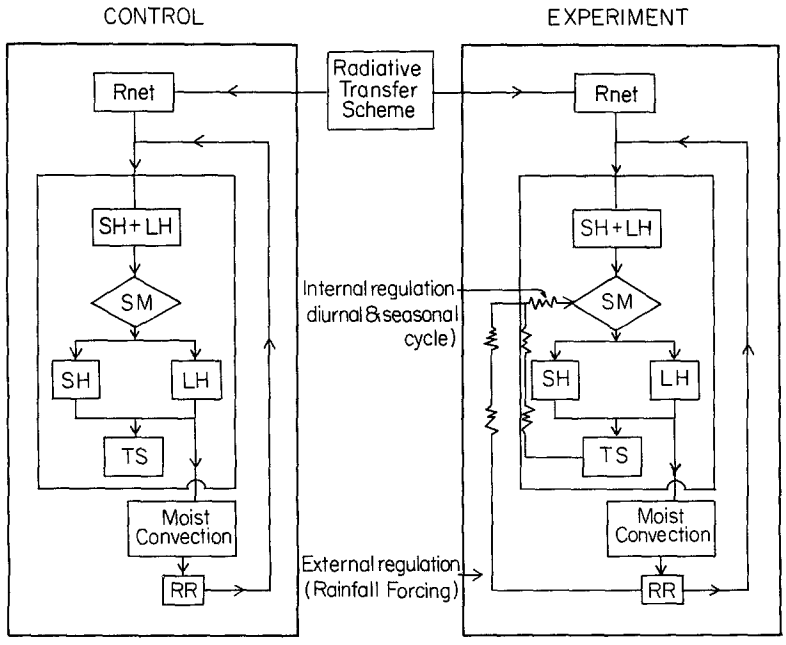

Fig. 10. Interaction between soil moisture and physical processes in the control and experiment (Rnet: net radiation, SH: sensible heat, LH: latent heat, SM: soil moisture, TS: surface temperature, RR: rainfall)

wetness of the ground and its temperature. But, the surface temperature itself is in turn determined by the net radiation and the ground wetness, since any excess energy, not balanced by evaporation and sensible heat or otherwise absorbed by the ground, forces an increase in the surface temperature. On the other hand, an increase in the surface temperature reduces the soil moisture availability. Therefore, any reduction in the incoming radiation is necessarily followed by a decrease in surface temperature and an increase in the soil moisture availability in the model. The available moisture at the ground is transferred to the PBL via turbulent fluxes and enhances moist convection. The resulting rainfall increases the soil moisture availability, which in turn will feed more moisture back into the PBL.

The dependence of the new soil moisture availability on surface temperature and rainfall resulted therefore in important interactions between the radiation, the moist convection, and the PBL parameterizations. The surface temperature appears to control the diurnal and seasonal cycles of the ground wetness parameter and represents an internal regulation inside the PBL. On the other hand, rainfall appears as an external regulator which forces the soil moisture availability's response to changes in the state of the ground induced by the moist convection scheme in the model. Both moist convection and the PBL interact coherently with the radiation scheme in the new surface energy balance.

It is to be noted that in nature the feedback between the different processes is continuous, while the update of the interaction between the soil moisture and rainfall in the model is done on a 24 hour basis. However, with respect to surface temperature, the ground wetness is updated at each time step.

7. Concluding Remarks

An assessment of the simulation of surface fluxes during a seasonal climate simulation using the FSUGSM has been described. A modification of the energy balance at the surface has been introduced to explicitly parameterize the heat transfer between the surface and the deep ground layer. Furthermore, a new parameterization of the soil moisture availability, which constitutes the central modulator in the partitioning of the energy at the land surface, has been implemented in a prognostic equation for surface temperature.

The examination of the different components of the surface energy budget at selected locations has revealed significant differences between the control and the experiment during all four months of the model integration. The incorporation of the soil heat flux at the land-atmosphere interface has reduced the energy available for sensible and latent heat fluxes. Its impact on the surface heat budget was to produce a more realistic evolution of the surface temperature with respect to its magnitude and diurnal range. This was particularly evident over arid and semi-arid regions, which were characterized by unrealistically high surface temperature maxima and extremely large diurnal cycle amplitudes during the control. A decrease in the maximum surface temperature of more than 6 °C, associated with a reduction of about 10 °C in the diurnal range, has been obtained during the warmest month over the African arid regions.

The introduction of the new soil moisture availability has resulted in an interesting modulation of the surface energy balance and produced smaller rates of surface evaporation. Except over the arid zones where small moisture flux components have been generated by the new scheme, systematic reduction of the soil moisture availability and its related evaporation flux have been observed over all considered types of climate in the absence of rain. During rainfall occurrence, however, the new soil moisture availability was larger than that prescribed in the control only over the tropical regions. It was found that over dry regions, the moisture fluxes predicted by this scheme were comparable to those produced by other similar GCMs and were also compatible with observations.

Through its formulation as a function of predictive variables, the new ground wetness parameter has shown interesting characteristics not present in the control. The effect of surface temperature has introduced diurnal and seasonal cycles in the soil moisture availability, while its dependence on predicted rainfall resulted in an important feedback between the model's physical mechanisms. Both the radiation and the convection have shown coherent interactions with the planetary boundary layer fluxes through the new formulation of the soil moisture availability.

Although not often experienced over the illus-

trated locations, the gradual decrease of the soil moisture parameter after the last fainfall occurrence occasionally enhanced convection and produced an effect close to what is normally observed in nature.

Unlike its counterpart in the control which is maintained constant, the new soil moisture parameter has introduced a realistic response to other physical processes in the model and has resulted in a remarkable partitioning of the surface energy fluxes. In the absence of rainfall, the soil moisture parameter showed relatively small values and maintained an energy balance with higher sensible heat fluxes. However, as clouds developed in the model and reduced the net incoming solar energy, the consequent reduction of the surface temperature increased the soil moisture parameter, supplying more moisture to the atmosphere. The resulting rainfall produced a significant increase in the soil moisture availability which had the double effect of increasing both the latent heat and ground heat fluxes. The consequent reduction of the Bowen ratio has contributed to an enhancement of moist convection.

The new soil moisture parameterization has also shown a realistic description of the West African monsoon surges over the Sahelian regions. When the monsoon moisture reached its northernmost position, a decrease in the net solar radiation reaching the ground led to a decrease in surface temperature and an increase in the ground wetness parameter over the considered area. Enhancement in the PBL moisture was then observed and was generally associated with important amounts of rainfall. An increase in the Bowen ratio was observed to be associted with dry spells over the region, as the monsoon winds withdrew.

The new surface energy balance parameterization has introduced the necessary feedback mechanism between the different elements controlling land surface processes, which was lacking in the FSUGSM. It is certain that albedo, rainfall and surface temperature are not the only parameters controlling the evolution of the soil moisture availability. Other elements describing the complex plant canopy are still necessary to fully describe the soil moisture-soil evaporation processes over land. The extreme sensitivity of surface temperature and rainfall to soil moisture availability suggests, however, that careful estimation of the latter be made when parameterizing the fluxes balance at the surface in a numerical model.

Appendix 1

List of Acronyms

BATS	Biosphere Atmosphere Transfer Scheme
FGGE	First GARP Global Experiment
FSUGSM	Florida State University Global Spectral Model
GARP	Global Atmospheric Research Program
GCM	General Circulation Model
GMT	Greenwich Mean Time
ITCZ	Intertropical Convergence Zone
MONEX	Monsoon Experiment
NMC	National Meteorological Center
OLR	Outgoing Longwave Radiation
PBL	Planetary Boundary Layer

References

Blackadar, A. K., 1979: High resolution models of the planetary boundary layer. In: Pfaffin, J., Zeigler, E. (eds.) *Advances in Environmental Science and Engineering 1*, No. 1. New York: Gordon and Breach Sci. Pub., pp. 50–85.

Blake, D. W., Krishnamurti, T. N., Low-Nam, S. V., Fein, J. S., 1982: The structure and energy budget of the heat flow over the empty quarter in Saudi Arabia during summer 1979. NORDA. Tech. Note 170, 46 pp [Available from code 322, NORDA, NSTL station, MS 39529].

Carson, D. J., Sangster, A. J., 1981: The influence of land-surface albedo and soil moisture on gerneral circulation model stimulation. In: Rutherford, I. D. (ed.) *Research Activities in Atmospheric and Oceanic Modelling.* Numerical Experimentation Program Report No. 2, pp. 5.14–5.21.

Charney, J. G., 1975: Dynamics of deserts and drought in the Sahara. *Quart. J. Roy. Meteor. Soc.*, **101**, 193–202.

Charney, J. G., Quirk, W. J., Chów, S. H., Kornfield, J., 1977: A comparative study of the effects of albedo change on drought in semi-arid regions. *J. Atmos. Sci.*, **34**, 1366–1385.

Chervin, R. M., 1979: Response of the NCAR general circulation model to changed land surface albedo. Report of the JOC Study Convergence on Climate Models: Performance, Intercomparison and Sensitivity Studies. GARP Publ. Series, No. 22, Vol. 1, 563–581.

Cunnington, W. M., Rowntree, P. R., 1986: Simulation of the Saharan atmosphere-dependence on mosture and albedo. *Quart. J. Roy. Meteor. Soc.*, **113**, 971–998.

Dastoor, Ashu, Krishnamurti, T. N., 1991: The landfall and structure of a tropical cyclone: the sensitivity of model predictions to soil moisture parameterization. *Bound.-Layer Meteor.*, **55**, 345–380.

Deardorff, J. W., 1972: Parameterization of the planetary boundary layer for use in general circulation models. *Mon. Wea. Rev.*, **100**, 83–106.

Dickinson, R. E., 1984: Modelling evapotranspiration for three dimensional global climate models. Geophysical monograph 29, A.G.U.

Gash, J. H., Wallace, J. S., Lloyd, C. R., Dolman, A. J., Sivakumar, M. V. K., Renard, C., 1991: Measurements of evaporation from follow Sahelian savanah at start of the dry season. *Quart. J. Roy. Meteor. Soc.*, **117**, 716–749.

Henderson-Sellers, A., 1980: The effects of land clearance and agricultural practices upon climate. *Blowing in the wind:*

Deforestation and long-range implications. Studies in Third World societies, Pub. No. 14, Department. Anthropology, College of William and Mary, 443–485.

Henderson-Sellers, A., Gornitz, V., 1984: Possible climatic impacts of land cover transformations, with particular emphasis on tropical deforestation. *Climatic Change,* **6**, 231–257.

Idso, S. B., Deardorff, J. W., 1978: Comments on the effect of variable surface albedo on the atmospheric circulation in desert regions. *J. Appl. Meteor.,* **17**, 560.

Krishnamurti, T. N., Sheng, J., 1984: FGGE IIIb (ECMWF) Vertical velocity tapes. FGGE IIIb Data Users. National Academy of Sciences, Newsletter 5. 12 pp [Available from USC GARP JH810, National academy of sciences, 2101 Constitution Ave. NW Washington D.C. 20418].

Krishnamurti, T. N., Kumar, A., Yap, K. S., Dastoor, A. P., Davidson, N., Sheng, J., 1990: Prediction of heavy tropical rainfall with a meso-scale model. *Adv. Geophys.,* **32**, 133–286.

Laval, K., Picon, L., 1986: Effect of change of the surface albedo on the Sahel Climate. *J. Atmos. Sci.,* **43**, 2418–2429.

Manabe, S., 1975: A study of the interaction between the hydrological cycle and climate using a mathematical model of the atmosphere. Report on meeting on weather-food interactions, Massachusetts Institute of Technology, 21–45.

Nitta, T., 1972: Energy budget of wave disturbances over the Marshall Islands during the years of 1956 and 1958. *J. Meteor. Soc. Japan,* **50**, 71–84.

Pan, Hua-Lu, 1990: A simple parameterization scheme of evapotranspiration over land for the NMC medium-range forecast model. *Mon. Wea. Rev.,* **118**, 2500–2512.

Rind, D., 1982: The influence of ground moisture conditions in North America on summer climate as modeled in the GISS GCM. *Mon. Wea. Rev.,* **110**, 1487–1494.

Rowntree, P. R., Bolton, J. A., 1983: Simulation of the atmospheric response to soil moisture anomalies over Europe. *Quart. J. Roy Meteor. Soc.,* **109**, 501–526.

Sellers, P. J., Dorman, J. L., 1987: Testing the simple biosphere model (SiB) using point micrometeorological and biophysical data. *J. Appl. Meteor.,* **26**, 622–651.

Shukla, J., Mintz, Y., 1982: Influence of land surface evapotranspiration on the earth's climate. *Science,* **125**, 1498–1501.

Sud, Y. C., Fennessy, M. J., 1982: A study of the influence of surface albedo on July circulation in semi arid regions using the GIAS GCM. *J. Climatol.,* **2**, 105–125.

Sud, Y. C., Smith, W. E., 1984: Ensemble formulation of surface fluxes and improvement in evapotranspiration and cloud parameterization in a GCM. *Bound.-Layer Meteor.,* **29**, 185–210.

Walker, J., Rowntree, P. R., 1977: The effect of soil moisture on circulation and rainfall in a tropical model. *Quart. J. Roy. Meteor. Soc.,* **103**, 29–46.

Yanai, M., Ebensen, S., Chu., J. H., 1973: Determination of bulk properties of tropical cloud clusters from large scale heat and moisture budgets. *J. Atmos. Sci.,* **30**, 611–627.

Yeh, T. C., Wetherland, R. T., Manabe, S., 1984: The effect of soil moisture on the short-term climate and hydrology change – A numerical experiment. *Mon. Wea. Rev.,* **112**, 474–490.

Authors' address: L. Bounoua and T. N. Krishnamurti, Department of Meteorology, Florida State University, Tallahassee, FL 32306, U.S.A.